



An Experimental Procedure to Estimate Surface Crack Density Using Thermography and Acoustic Emissions

Rosa De Finis¹(✉), Davide Palumbo¹, Umberto Masone²,
Marilena Doriana D'addona³, Roberto Teti³, and Umberto Galietti¹

¹ Politecnico di Bari, Bari, Italy
rosa.definis@poliba.it

² TUV Austria-Italia – Blu Solutions srl, Monte Roberto, Italy

³ Department of Chemical, Materials and Industrial Production Engineering, University of
Naples Federico II, Naples, Italy

Abstract. The current study discusses two aspects of an infrared thermography-based local SHM system for monitoring damage evolution during fatigue of composites materials, namely, pre-macrocrack damage (Stage I) followed by subsequent crack growth (Stage II).

The crack density is a very well-known damage parameter representing the actual mechanical state of the material in terms of stiffness degradation. In effect, for laminates presenting off-axis laminae, crack density is useful for determining the “characteristic damage state” (CDS) that is related the load carrying capability of the laminate.

In present research, a novel procedure is proposed for performing contactless measurements of crack density during static tensile tests by using temperature signal.

The results have been critically compared with the strain waves signal acquired by acoustic emission sensors during the same tests. The proposed technique and procedure lead to estimate the crack density in those applications where it is difficult to detect transverse crack using a direct measurement from common experimental techniques.

Keywords: Thermography · Acoustic emission · Structural health monitoring · Transverse crack density · Characteristic Damage State

1 Introduction

The anisotropy and heterogeneity of composites influence unavoidably the mechanical response of the material to external excitation and the failure mechanisms [1–6].

As an effect, the mechanical behaviour assessment of composites requires to pay attention to the influence of the specific layup of laminae, viscous properties of the matrix, pattern described by the yarns or fibers. In general, damage in composites is characterized by the occurrence of specific damage stages of different mechanisms [3–5]. The transverse cracks are typical of a first damage stage while delamination and

fiber breakage are specific of the second and the third stages. A specific damage state occurs during the delamination regime, where the damage achieves a fixed value called Characteristic Damage State (CDS) [6–8]. The CDS is important to understand the material damage progression [9, 10].

It follows that specific quantitative and qualitative analyses are required for the data processing in order to carry out an efficient SHM. In effect, to evaluate the structural health of the material an appropriate damage parameter is transverse cracks [9–14], that is also related to the material mechanical properties degradation [15, 16]. The major difficulties in the experimental evaluation of the crack number are related to the identification of the cracks and in the evaluation of the crack length [14] coupled with a complex setup and suitable material preparation.

The adopted techniques to measure the transverse cracks number are the optical microscopy [12] and acoustic emission techniques [17]. Acoustic emissions AE is the well-established technique, widely used to detect and identify damage mechanisms in composites. In particular, different studies were set up to try to establish a link between damage mechanisms in composites and the related acoustic emission using empirical correlations between the signal and the source mechanism [18–23].

Another interesting technique that is showing its capability in the qualitative and quantitative damage assessment is the infrared thermography [2, 3]. Thermography is, in effect, successfully adopted to estimate the surface crack density during cyclic loading, and the results matched very well those provided by analytical models [3] however the comparison between crack density measured by Infrared thermography and the one measured by a well-established technique has not been presented yet.

In recent years, AE were combined with infrared thermography [24] or digital image correlation [25] to estimate the damage, even if, few validations for the findings from these techniques labelling damage mechanisms of the AE source are provided [26, 27].

In this way, in the present work, the surface crack density estimated during a static test is compared to the crack density measured by AE. The results, show as the thermal signal analysis is capable of estimating the surface transverse cracks number of a quasi-isotropic CFRP composite obtained by Automated Fiber Placement under static tensile loading in a good agreement with AE. The preliminary presented results pave the way towards the definition of a new procedure based on infrared thermography to implement the SHM of CFRP composites, of course more investigations are required for validating the thermographic data using AEs.

2 Theory: Temperature-Related Sentinels of Damage

In presence of small thermal gradient conditions through the thickness, the direct link between local heat sources and the surface temperature fields discussed by several authors [28] is described by:

$$dC_\varepsilon \frac{\partial \vartheta}{\partial t} - \left[k_{xx} \frac{\partial^2 \vartheta}{\partial x^2} + k_{yy} \frac{\partial^2 \vartheta}{\partial y^2} + k_{zz} \frac{\partial^2 \vartheta}{\partial z^2} \right] = \varphi_{int} + s_{the} \quad (1)$$

Under specific assumptions [29] on material state, test procedure, Eq. 1 represents the local heat diffusion equation where $\vartheta = T - T_0$ is the temperature variation between

the current state, T , and an initial state T_0 , d is the material density (ρ symbol is avoided), C_ε is the specific heat capacity at constant strain, $k_{xx,yy,zz}$ are the thermal conductivity tensor terms.

In Eq. 1 φ_{int} , is the intrinsic dissipation that is the volume rate of mechanical energy dissipated as heat (directly related to damage [30–32]) and the term s_{the} represents the thermoelastic reversible heat source. The sum of these latter is the total volume heat source.

More generally, intrinsic dissipations are due to internal frictions caused by visco-elastic behaviour of the matrix [5, 6, 9], cracks that produce a variation in the material internal energy and a reduction of the loading bearing capability [14, 16]. In presence of cracks, φ_{int} represents also the energy spent for the creation of crack new surfaces according to Griffith's theory [33]. In addition, when damage involves delamination between cracked/un-cracked layers, internal friction occurs producing an energy increase [29].

In last decades, some researchers were focused on investigating temperature variations related to reversible and irreversible heat sources [2–4, 30–32].

In particular, the superficial temperature variations during fatigue damage cycles present a characteristic behaviour over the time: a mean temperature growth with a superimposed periodic temperature variation due to the cyclically imposed load. So that, temperature can be used as damage sentinel.

The effect of damage on the temperature signal can be investigated by comparing damaged and undamaged conditions. Following this, it can be assumed that in a region where the composite experiences a damage mechanism such as a crack, there will be concurrent mechanisms affecting both reversible and irreversible heat sources, and then influencing the mean temperature and its harmonic components [30–32]. In this way, temperature can be useful to detect the energy-related phenomena accompanying crack appearance [2–4].

Accounting for the work [2], in present research the crack density measured by infrared thermography using the procedure presented will be compared with the crack density obtained by the well-established acoustic emission technique in order to confirm the capability of IR-Thermography to detect and estimate transverse cracks.

3 Experimental Campaign

Automatic Fiber Placement technology is an innovative technology aimed at depositing composite layers as unidirectional prepreg tapes [3]. The tested material is a quasi-isotropic CFRP with a layup of $[0/-45/45/90/90/45/-45/0]_2$. The cut direction of the specimens coincides with 90° -layers orientations. So that, for the specimens the outer layer is oriented in 90° direction to the load applied.

Sample dimensions are 25 mm width, 250 mm length and 3.0 mm thick. All the specimens are tested on servo-hydraulic loading frame INSTRON 8850 (250 kN capacity).

Three samples were addressed to static tensile tests at 1 mm/min of displacement rate according to the Standard [22]. The obtained ultimate tensile strength (UTS) of material is 825 MPa (standard deviation 84.57 MPa). One test was monitored using both IR

camera FLIR X6540 SC that acquired at a frequency of 75 Hz and two AE piezoelectric sensors (S1–S2, resonant frequency 150 kHz). Typical damage mechanisms [27] occur in the frequency range of 50–200 Hz.

Figure 1 describes the setup and layout of the adopted equipment.

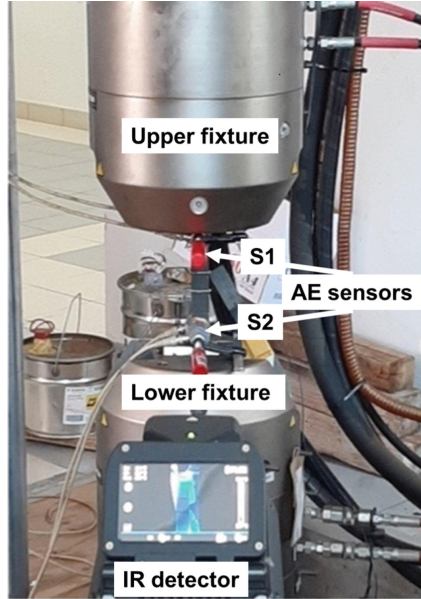


Fig. 1. Equipment and layout

4 Methods and Data Processing of Thermal Data

The thermal signal data from tensile tests have been processed by using a specific procedure allowing to filter out the signal from material pattern and enhancing the signal from cracks. In effect, the measured data from the infrared detector require a specific processing procedure as they are affected by thermal gradients through the sample, material fabric pattern etc....

In Fig. 2a, the temperature map of sample 1 is represented together with the sample in the visible-band where the transverse cracks are visible. The two images of Fig. 2a correspond to two different time instants (halfway of the test duration for temperature map and close to failure for the one in the visible-band).

The infrared thermal map presents not only an increase of temperature in proximity of the upper fixture that was imposing the monotonically increasing deformation, but also in lower part caused by hot oil from loading machine fixture and friction between AE sensor and sample. This leads to some issues in evaluating the cracks occurring in the matrix as the total gradient through the sample is basically higher than the temperature variation associated to a crack.

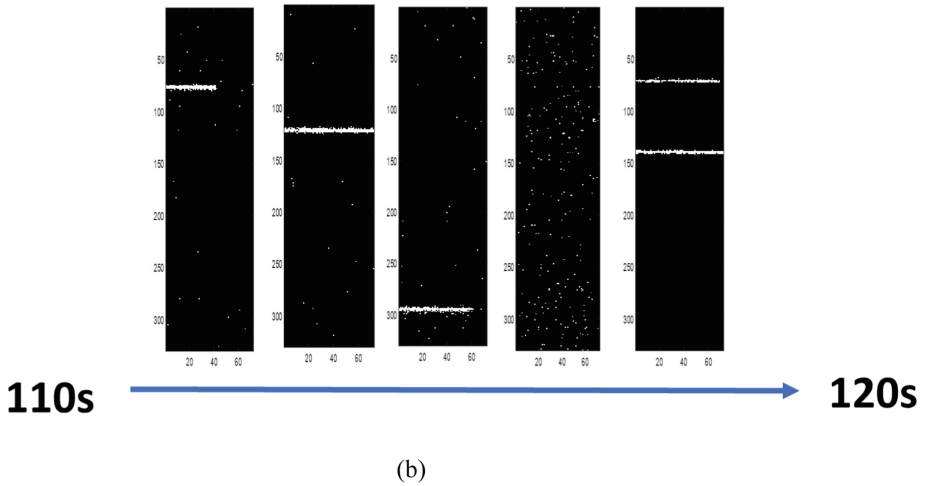
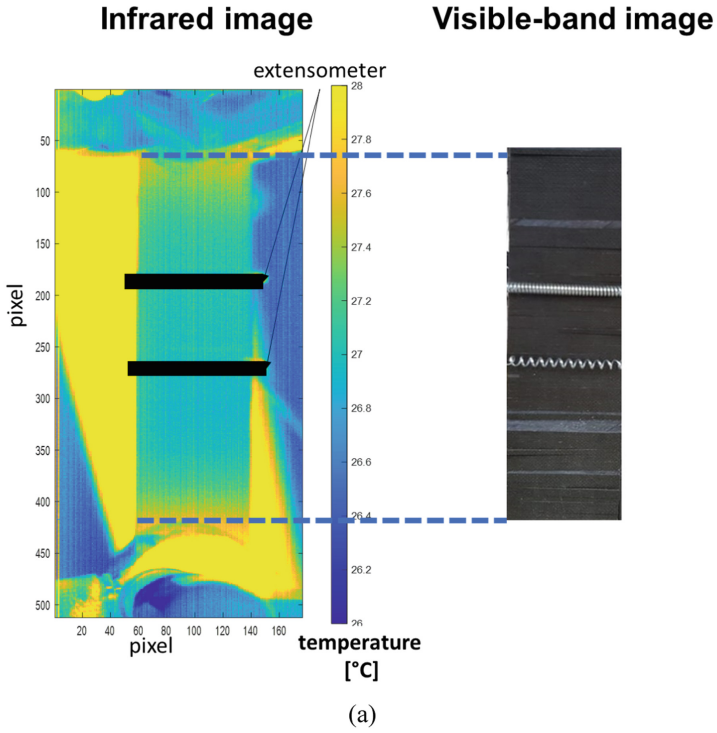


Fig. 2. (a) temperature map acquired halfway through the test duration and visible-band image acquired close to failure of sample 1, (b) binarized maps where transverse cracks (white bands crossing the sample) are detected.

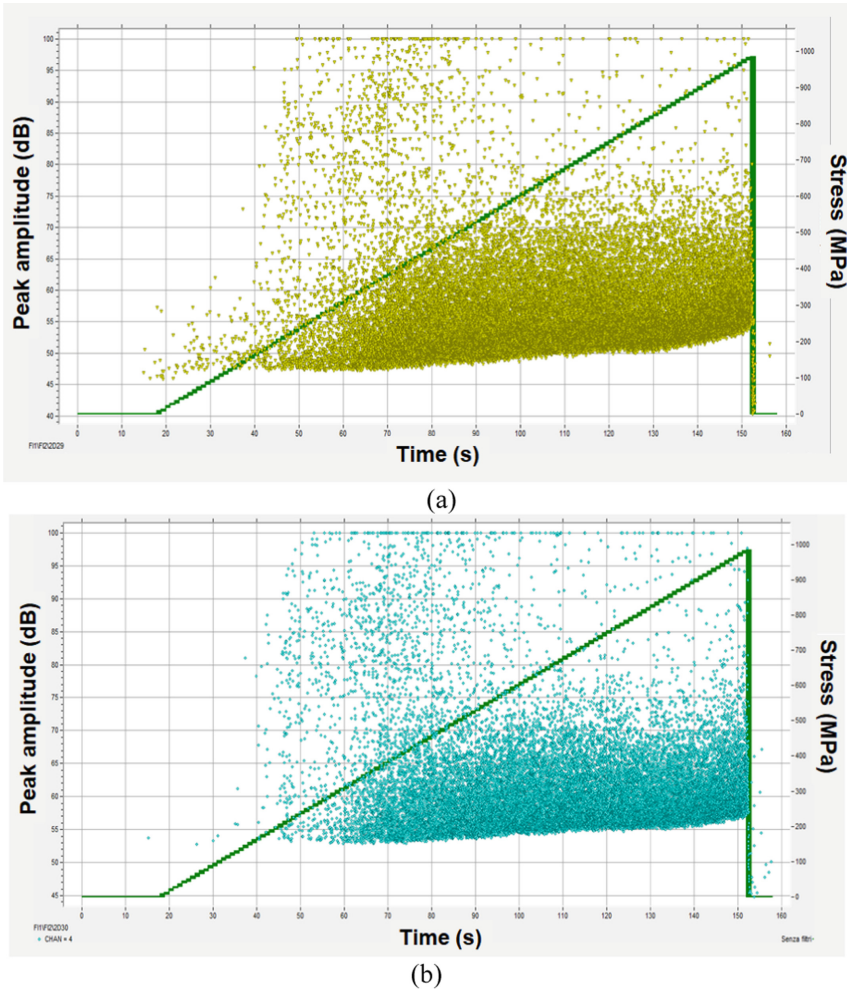
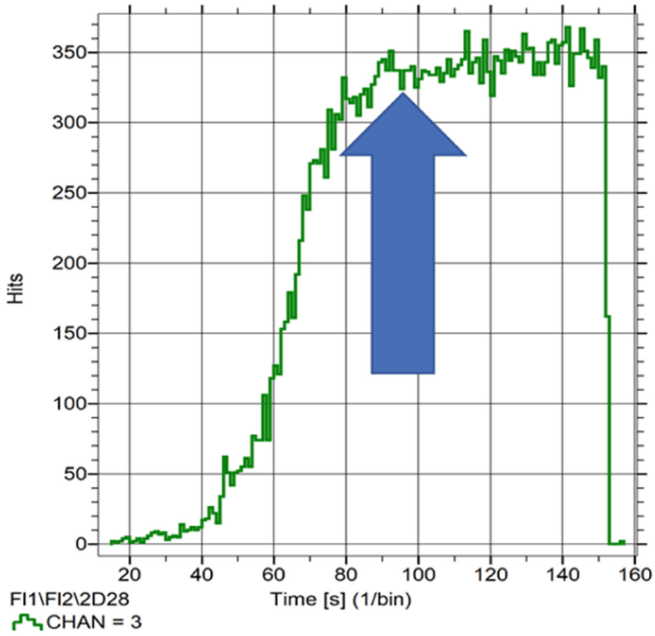


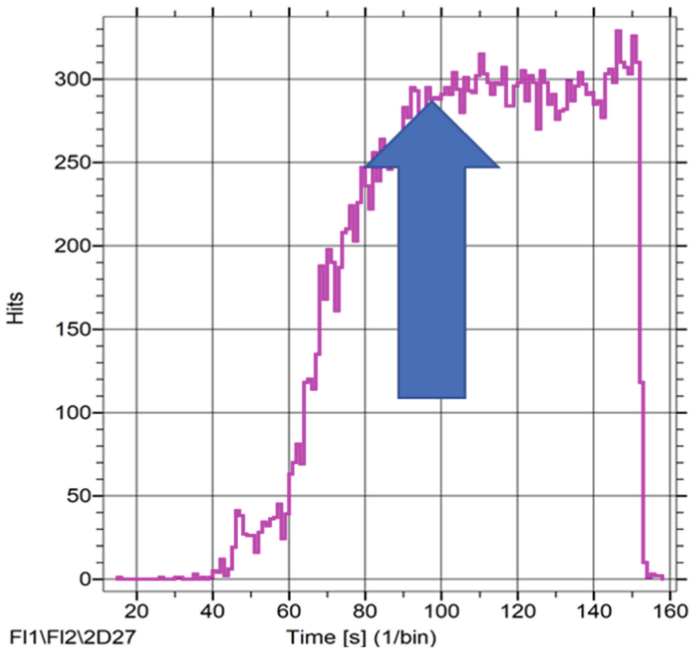
Fig. 3. Peak amplitude and stress versus time for (a) sensor 1, (b) sensor 2.

In this way, as described in [2], a Matlab® code was developed to operate on temperature tridimensional matrixes (each pixel value represented the temperature value at specific time instant) in order to subtract from each matrix at a specific time instant the data matrix from previous time instant (dynamic frame subtraction). According to the work [2] the cracks were assessed, Fig. 2b.

The maps in Fig. 2b, in particular, report the detected transverse cracks during static tensile test between 110th and 120th second of the thermal sequence. The maps are the output of a binarization process of converting a pixel image to a binary image after a threshold gets applied [2].

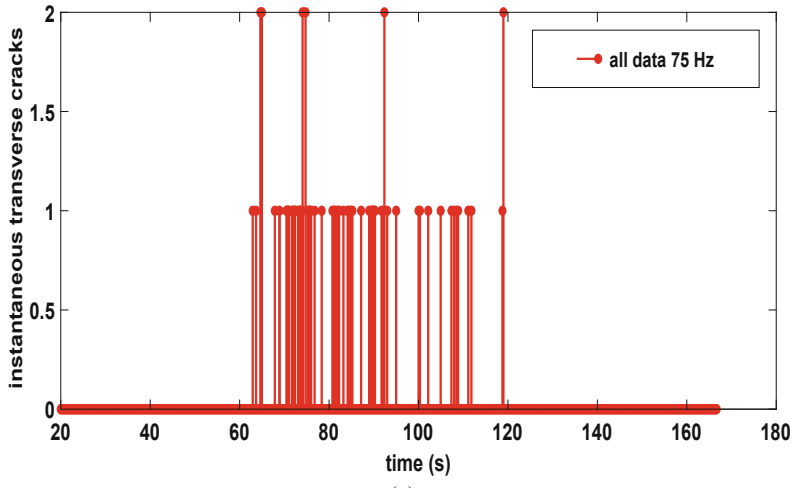


(a)

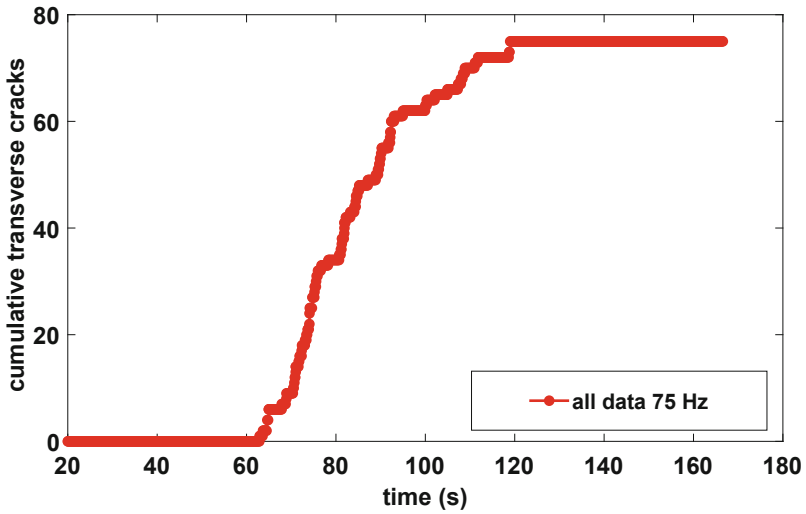


(b)

Fig. 4. Hits for (a) sensor 1, (b) sensor 2.



(a)



(b)

Fig. 5. Crack number during static tests: (a) instantaneous, (b) cumulated.

5 Results and Discussion

In this section the results in terms of crack number are evaluated for the sample 1 in terms of surface transverse cracks detected using thermography and crack density using AEs.

5.1 Acoustic Emission Results

As for the acoustic emissions Fig. 3 shows the peaks and stress evolution measured by sensor 1 (S1) and sensor 2 (S2).

As a general consideration, it is possible to highlight that the peak events start immediately few instants after the test started, as the stress increase, specifically peaks starts after 20 s in the upper region (S1) and after 40 s in the lower region (S2), as expected. In effect, for composites the damage starts as the stress is imposed in a continuous damage progression. In the same Fig. 3, it is possible to observe that it is necessary a post processing analysis to filter out the signal from damage (transverse cracks) and noise. Moreover, another interesting observation is such that the damage events seems to start before on upper region than in lower region, this can be explained by considering that upper region, where S1 is positioned, is near moving fixture, and then the motion of the fixture can allow a more intense activity.

Figure 4, shows the hits on S1 (Fig. 4a) and S2 (Fig. 4b). In both of figures the number of hits is slightly different: higher the number of events hitting S1 (near moving fixture) than those on S2. However, the hits behaviour is similar for both S1–2 and after a lower activity, the hits proceed until a steady state is achieved: the characteristic damage state [12, 13]. Such a point has been also indicated by an arrow.

5.2 Crack Density from Infrared Thermography

In Fig. 5 are represented the number of instantaneous (Fig. 5a) and cumulated cracks (Fig. 5b) assessed during the static tensile tests. The number of instantaneous cracks appearing through the sample during the test is clearly discontinuous and starts at a specific moment after the test start (60 s). This can be explained by considering that the thermography is a surface/subsurface technique, its screening is limited to surficial layers, so that the cracks counted are those of the initial layers. However, by observing the Fig. 5b it is also interesting to observe that before the final failure there is the ‘characteristic damage state’ (CDS). In general, depending on the material, CDS for static tests is different from the one found during fatigue [9, 10]. This indicates that the technique can be a useful tool to estimate the damage parameter.

6 Conclusions

In this work, a quasi-isotropic CFRP sample made by automated fiber placement was tested under static loading. The tests were assisted by an infrared camera and acoustic emission sensors.

The surface crack density trend measured by infrared thermography is in agreement with the one measured by AEs. Of course, cracks estimated by using thermal signal are just an estimation of those provided by the well-established technique.

The results demonstrated the capability of the infrared thermography to detect and estimate the crack number and then the capability of studying damage during any kind of loading. This approach seems to be promising for those applications where it is difficult to measure the crack length or to apply AE sensors.

Further investigations will focus on relating the transverse cracks from AEs and those from thermography depending on specific material.

Acknowledgements. This work is part of a R&D project “SISTER CHECK – Sistema Termografico prototipale per il controllo di processo, la verifica e la caratterizzazione di materiali avanzati per l’aerospazio” – of the research program “Horizon 2020” PON I&C 2014- 2020 call. The authors would like to thank Diagnostic Engineering Solutions Srl, Novotech Aerospace Advanced Technology S.R.L. for the manufacturing of the samples and Professor Riccardo Nobile and Eng. Andrea Saponaro for the support during the experimental activity performed in this work.

References

1. Bannister, M.K.: Development and application of advanced textile composites. *Proc. Inst. Mech. Eng. Part L: J. Mater. Des. Appl.* **218**, 253–260 (2004)
2. De Finis, R., Palumbo, D., Galietti, U.: Infrared thermography to study damage during static and cyclic loading of composites. *Lect. Notes Civ. Eng.* **128**, 309–318 (2021)
3. De Finis, R., Palumbo, D., Galietti, U.: An experimental procedure based on infrared thermography for the assessment of crack density in quasi-isotropic CFRP. *Eng. Fract. Mech.* **258**, 108108 (2021)
4. Huang, J., Pastor, M.J., Garnier, C., Gong, X.J.: A new model for fatigue life prediction based on infrared thermography and degradation process for CFRP composite laminates. *Int. J. Fatigue* **120**, 87–95 (2019)
5. Degrieck, J., Van Paepegem, W.: Fatigue damage modeling of fibre-reinforced composite materials: review. *Appl. Mech. Rev.* **54**(4) (2001)
6. Hashin, Z.: Analysis of composite materials. *J. Appl. Mech.* **50**, 481 (1983)
7. Stens, C., Middendorf, P.: Computationally efficient modelling of the fatigue behaviour of composite materials. *Int. J. Fatigue* **80**, 69–75 (2015)
8. Renard, J., Favre, J.P., Jeggy, T.H.: Influence of transverse cracking on ply behavior: introduction of a characteristic damage variable. *Compos. Sci. Technol.* **46**, 29–37 (1993)
9. Pakdel, H., Mohammadi, B.: Prediction of outer-ply matrix crack density at saturation in laminates under static and fatigue loading. *Int. J. Solids Struct.* **139**, 43–54 (2018)
10. Luterbacher, R., Trask, R.S., Bond, I.P.: Static and fatigue tensile properties of crossply laminates containing vasculcs for selfhealing applications. *Smart Mater. Struct.* **25**, 015003 (2016)
11. Gamby, D., Rebière, J.L.: A two-dimensional analysis of multiple matrix cracking in a laminated composite close to its characteristic damage state. *Compos. Struct.* **25**, 325–337 (1993)
12. Pakdel, H., Mohammadi, B.: Stiffness degradation of composite laminates due to matrix cracking and induced delamination during tension-tension fatigue. *Eng. Fract. Mech.* **2019**, 216 (2019)
13. Okabe, T., Onodera, S., Kumagai, Y., Nagumo, Y.: Continuum damage mechanics modeling of composite laminates including transverse cracks. *Int. J. Damage Mech.* 1–19 (2017)
14. Talreja, R., Varna, J.: *Modeling Damage, Fatigue and Failure of Composite Materials*, vol. 65. Woodhead Publishing Series in Composites Science and Engineering (2016)
15. Ogin, S.L., Smith, P.A., Beaumont, P.W.R.: Matrix cracking and stiffness reduction during the fatigue of a (0/90)s GFRP laminate. *Compos. Sci. Technol.* **22**, 23–31 (1985)
16. Carraro, P.A., Quaresimin, M.A.: stiffness degradation model for cracked multidirectional laminates with cracks in multiple layers. *Int. J. Solids Struct.* **58**, 34–51 (2015)

17. Tsamtaskis, D., Wevers, M., De Meester, P.: Acoustic emission from CFRP laminates during fatigue loading. *J. Reinf. Plastics Compos.* **17** (1998)
18. Van Hemelrijck, D., Anastassopoulos, A.A.: *Non Destructive Testing*. Balkema, Rotterdam (1996). ISBN 905410595
19. Anastassopoulos, A., Philippidis, T.P.: Clustering methodology for the evaluation of acoustic emission from composites. *J. Acoust. Emiss.* **13**, 11–12 (1995)
20. Ramasso, E., Placet, V., Boubakar, M.L.: Unsupervised consensus clustering of acoustic emission time-series for robust damage sequence estimation in composites. *IEEE Trans. Instrum. Meas.* **64**, 3297–3307 (2015)
21. Morscher, G.N., Godin, N.: *Use of Acoustic Emission for Ceramic Matrix Composites*, pp. 569–590. Wiley, Hoboken (2014)
22. Alia, A., Fantozzi, G., Godin, N., Osmani, H., Reynaud, P.: Mechanical behaviour of jute fibre-reinforced polyester composite: characterization of damage mechanisms using acoustic emission and microstructural observations. *J. Compos. Mater.* **53**, 3377–3394 (2019)
23. Guel, N., et al.: Data merging of AE sensors with different frequency resolution for the detection and identification of damage in oxide-based ceramic matrix composites. *Materials* **13**, 4691 (2020)
24. Li, L., Lomov, S.V., Yan, X.: Correlation of acoustic emission with optically observed damage in a glass/epoxy woven laminate under tensile loading. *Compos. Struct.* **123**, 45–53 (2015)
25. Munoz, V., et al.: Damage detection in CFRP by coupling acoustic emission and infrared thermography. *Compos. Part B Eng.* **85**, 68–75 (2016)
26. Godin, N., Reynaud, P., Fantozzi, G.: Challenges and limitations in the identification of acoustic emission signature of damage mechanisms in composites materials. *Appl. Sci.* **8**, 1267 (2018)
27. Gutkin, R., Green, C.J., Vangrattanachai, S., Pinho, S.T., Robinson, P., Curtis, P.T.: On acoustic emission for failure investigation in CFRP: pattern recognition and peak frequency analyses. *Mech. Syst. Sig. Process.* **25**, 1393–1407 (2011)
28. Enke, N.F., Sandor, B.I.: Cyclic plasticity analysis by differential infrared thermography. In: *Proceeding of the VII International Congress on Experimental Mechanics*, pp. 830–835 (1988)
29. Lisle, T., Bouvet, C., Pastor, M.L., Margueres, P., Corral, P.: Damage analysis and fracture toughness evaluation in thin woven composite laminate under static tension using infrared thermography. *Compos. A* **53**, 75–87 (2013)
30. De Finis, R., Palumbo, D., Galietti, U.: A multianalysis thermography-based approach for fatigue and damage investigations of ASTM A182 F6NM steel at two stress ratios. *Fatigue Fract. Eng. Mater. Struct.* **42**(1), 267–283 (2019)
31. Sakagami, T., Kubo, S., Tamura, E., Nishimura, T.: Identification of plastic-zone based on double frequency lock-in thermographic temperature measurement. In: *International Conference of Fracture ICF11 2015, Catania (Italy)* (2015)
32. Krapez, J.K., Pacou, D., Gardette, G.: Lock-In Thermography and Fatigue Limit of Metals. *Quantitative Infrared Thermography, QIRT*, 18–21 July 2000, Reims (France) (2000)
33. Robert, L., Mecholsky, J., Freiman, W.: Estimation of fracture energy from the work of fracture and fracture surface area: I. Stable crack growth. *Int. J. Fract.* **156**, 97–102 (2009)